nature physics

SUPPLEMENTARY INFORMATION

DOI: 10.1038/NPHYS1223

SUPPLEMENTARY INFORMATION
for "The Quantum-Optical Josephson Interferometer"

D. Gerace,[1,2] Hakan E. Türeci,[1] A. Imamoglu,[1] V. Giovannetti,[3] and Rosario Fazio[3,4]

[1] *Institute of Quantum Electronics, ETH Zurich, 8093 Zurich, Switzerland*
[2] *CNISM and Dipartimento di Fisica "A. Volta," Università di Pavia, 27100 Pavia, Italy*
[3] *NEST (CNR-INFM) and Scuola Normale Superiore, Piazza dei Cavalieri 7, 56126 Pisa, Italy*
[4] *International School for Advanced Studies (SISSA), via Beirut 2 − 4, 34014 Trieste, Italy*

1 Experimental feasibility

In the main text we have considered a generic Kerr nonlinearity as the source of strong photon correlation in the central cavity. A possible way of experimentally implementing an effective hamiltonian of the type (1) or (5) in the main text is to couple 4-level atomic ensembles with microtoroid resonators, as described in detail in the literature [1]. The latter certainly represents an interesting possibility for a practical realization of our proposal with state-of-the art atomic cavity QED. Our focus here will be on the scheme represented in Fig. 1b and d (see text), in which a quantum dot (QD) is assumed to be deterministically coupled to the high-Q photonic crystal cavity mode in the middle [2]. It has been experimentally shown that such a system displays single-photon nonlinearities under coherent resonant pumping [3]. Photonic crystal (PC) circuits allow for a straightforward on-chip implementation with side-coupled cavities (as in Fig. 1b) or waveguides (as in Fig. 1d). If the hopping parameter J is small compared to the laser intensities $|E_1|$ and $|E_3|$, we can approximate the states of the external cavities with coherent fields of intensity $2|E_{1,3}|/\gamma$ (with γ being the damping parameter of the external cavities). Thus, to first order in $J/|E_{1,3}|$, the dynamics of the central cavity can be effectively described by replacing in the Hamiltonian the operators $\hat{p}_1$ and $\hat{p}_3$ with $2|E_{1,3}|/\gamma$, with reference to the derivation of the model in Eq. (5) in the text. With this choice the 3-cavity set-up can be effectively reduced to a Jaynes-Cummings model coupled to external driving fields and described by the simplified model

$$\hat{H} \sim \Delta_c \hat{a}_2^\dagger \hat{a}_2 + \Delta_x \hat{\sigma}_+ \hat{\sigma}_- + ig(\hat{a}_2^\dagger \hat{\sigma}_- - \hat{\sigma}_+ \hat{a}_2) + E_{\rm eff} \hat{a}_2^\dagger + E_{\rm eff}^* \hat{a}_2 \,, \tag{S1}$$

where $\hat{a}_2$ ($\hat{a}_2^\dagger$) represents annihilation (creation) of cavity photons, while $\hat{\sigma}_-$, and $\hat{\sigma}_+$ are Pauli lowering and rising operators related to the effective two-level system representing the QD exciton transition; $g = \hbar(\pi e^2 f/\varepsilon m^* V_{\rm eff})^{1/2}$ is the exciton-photon coupling (expressed in terms of the effective cavity mode volume and the QD oscillator strength) [4], and $\Delta_c = \omega_c - \omega_{\rm L}$ and $\Delta_x = \omega_x - \omega_{\rm L}$ are the cavity and exciton detuning from the pump frequency, respectively. The effective pumping strength is $|E_{\rm eff}| \propto |E_1 + E_2|/\gamma$ and is responsible for the effects of phase detuning, $\phi = \phi_1 - \phi_3$.

To give some numbers, state-of-the art solid state QED with GaAs-based materials allows for $Q \sim 10^5 - 10^6$, i.e. realistic $\gamma_c \sim 0.01$ meV [5], $\gamma_x \sim 1.3 \times 10^{-3}$ meV [6], $g = 0.11$ meV [2]. In the experiment, g is fixed as well as J, but the effective single-photon nonlinearity can be tuned by changing $\delta = \omega_x - \omega_c$. There are a number of different techniques to deterministically tune the cavity mode frequency [2, 7, 8, 9] and/or the QD exciton resonance [10]. For the system excitation, the same laser source can be sent through a beam-splitter, one of the arms going directly into the PC circuit (e.g. through a tapered access waveguide) with phase ϕ_1,

DOI: 10.1038/NPHYS1223

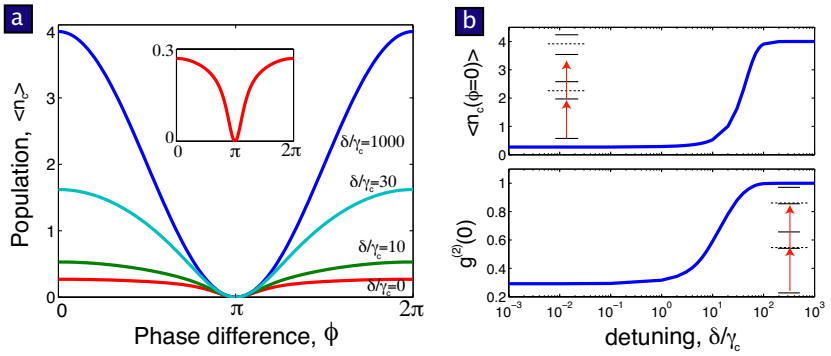

Figure S1: Numerical simulation of a realistic model with a JC-type non-linearity. We assume parameters of the model in Eq. (S1) $g/\gamma_c = 10$, $g/\gamma_x = 100$ (realistically achievable parameters, see text), and effective pumping strength $|E_{\rm eff}|/\gamma_c = 1$ at $\phi = 0$. Results are shown for light intensity and second-order correlation function emitted from the middle cavity, i.e. $\langle n_c\rangle = \langle \hat{a}_2^\dagger \hat{a}_2\rangle$ and $g^{(2)}(0) = \langle \hat{a}_2^\dagger \hat{a}_2^\dagger \hat{a}_2 \hat{a}_2\rangle / \langle n_c\rangle^2$. (a) Josephson-like oscillations are suppressed when the cavity-exciton detuning $\delta \to 0$. When $\delta \gg \gamma_c, g$, i.e. the exciton resonance is strongly blue-detuned from the cavity mode, the lower polariton is more and more cavity-like, hence the effective nonlinearity of the system is tuned through adjusting δ. In the inset, a zoom on the curve for $\delta = 0$. (b) The crossover from correlated to delocalized regimes is shown for $\langle n_c\rangle$ and $g^{(2)}(0)$ at $\phi = 0$, respectively, as a function of δ.

while the other being delayed and sent through a second tapered waveguide into the circuit with phase ϕ_3. Given that lasers with sub-MHz linewidth (i.e. much smaller than cavity and exciton dissipation rates) are currently available, we do not regard possible phase fluctuations in the two driving fields as a limiting issue for this scheme to be realized. Finally, it is key to this experiment that the pump laser frequencies be tuned to the lower polariton frequency of the JC spectrum, i.e. for each detuning δ we set $\omega_{\rm L} \simeq (\omega_x + \omega_c)/2 - \sqrt{g^2 + \delta^2/4}$ [2].

We simulate this model by solving the corresponding master equation that incorporates realistic cavity and exciton dissipation rates. Figure S1 shows that the predictions of the Jaynes-Cummings model in Eq. (S1) are qualitatively similar to the ideal Kerr nonlinearity model of Eq. (5) in the main text. In particular, the dependence of light intensity on ϕ shows suppression of Josephson-like oscillations as the exciton frequency is tuned (from the blue-side) in resonance with the cavity mode. The increase of the amplitude of oscillations towards the bare-cavity limit appears together with a crossover from sub-Poissonian to Poissonian statistics as a function of δ, consistent with the results of Fig. 3 in the main text. Here, tuning δ is a way of effectively tuning the nonlinearity in the central cavity, and thereby to experimentally observe the crossover from tunnel-coupled to strong correlated photon dynamics in a state-of-the art device. Notice that the linear regime is completely recovered for $\delta/\gamma_c \simeq 100$, i.e. $\delta \sim 1$ meV with the parameters given above, which is perfectly within reach of present experimental capabilities. In order to compare the behaviour of the different models, we notice that the strongly correlated limit of Fig. S1a ($\delta = 0$, curve in the inset) is qualitatively similar to the result obtained with a Kerr nonlinear model, Eq. (5) in the text, for $2U = (2 - \sqrt{2})g$, i.e. $U/\gamma_2 \simeq 3$, as it is shown in Fig. S2a and its inset. The crossover

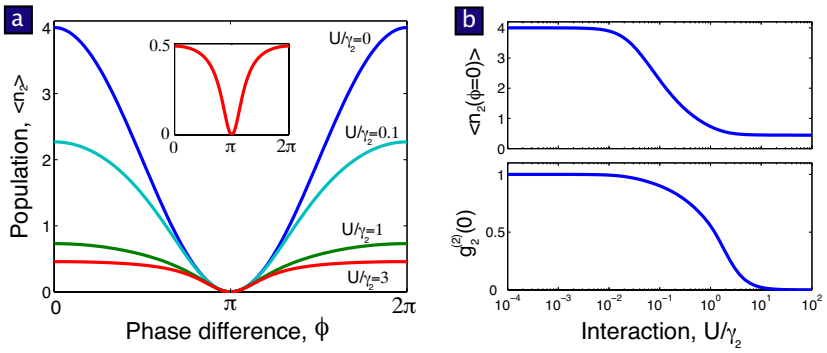

Figure S2: Numerical simulation for the model of Eq. (5) in the main text with effective pumping strength $|E_{\rm eff}|/\gamma = 1$ at $\phi = 0$. (a) Josephson-like oscillations are suppressed on increasing the effective Kerr nonlinearity, U/γ_2. In the inset, a zoom on the curve for $U/\gamma_2 = 3$, to be compared to the previous figure. (b) Crossover from correlated to delocalized regimes for $\langle n_2 \rangle$ and $g_2^{(2)}(0)$ at $\phi = 0$, respectively, as a function of U/γ_2.

from delocalized to localized regimes as a function of U is shown in Fig. S2b to be compared to Fig. S1b. We note that the correspondence between a generic Kerr-type non-linearity studied in the main text and a JC-like non-linearity studied here is strictly valid only in the low-pumping regime.

The same model and experimental approach can be used to study the realization of the quantum optical Josephson interferometer based on different technologies, such as circuit QED [11] or quantum well exciton-polaritons. While there is no experimental evidence of Kerr nonlinear behaviour of 3D confined cavity polaritons at time of writing, it is likely that polariton blockade in a single quantum box can be achieved in the near future along the lines and numbers quoted in the literature [12], e.g. with an alternative cavity geometry recently realized [13]. Such a result would make possible a more *direct* realization of our model with a Kerr nonlinearity in the solid state.

2 Derivation of Eq. (4)

Here we investigate the steady state dynamics of the Hamiltonian (7) in the weak pumping limit. We present here a derivation of the expressions for $\langle n_2(\phi = 0)\rangle$ and $g_2^{(2)}(\tau = 0) = \langle \hat{p}_2^\dagger \hat{p}_2^\dagger \hat{p}_2 \hat{p}_2 \rangle / \langle n_2 \rangle^2$. Consider the low-energy excitations of the Hamiltonian (7) in the basis $|n_2, n_s\rangle$ where $N_{tot} = n_2 + n_s$ is the total number of photons. In the weak pumping limit, the driving term $\tilde{E}\hat{s}^\dagger + \tilde{E}^* \hat{s}$ causes transitions between the manifolds N_{tot} and $N_{tot} + 1$. Let us write the total time-dependent wavefunction of the system as $\Psi(t) = \sum_n a_n |n\rangle$. In the weak pumping limit, we consider the lowest three total photon manifolds $N_{tot} = 0, 1, 2$, hence $n = 0, \ldots, 5$. The corresponding energy level diagram and the rates are shown in Fig. S3.

Terms neglected in $\Psi(t)$ will be of order $O(\frac{|\tilde{E}|}{\bar{\gamma}})^3$ where $\bar{\gamma}$ is the typical decay rate of the system (γ_2, γ). It's important to write the equations of motion in the bare basis instead of the basis of the coupled cavity states to get the dissipation rates correctly. The equations of

DOI: 10.1038/NPHYS1223

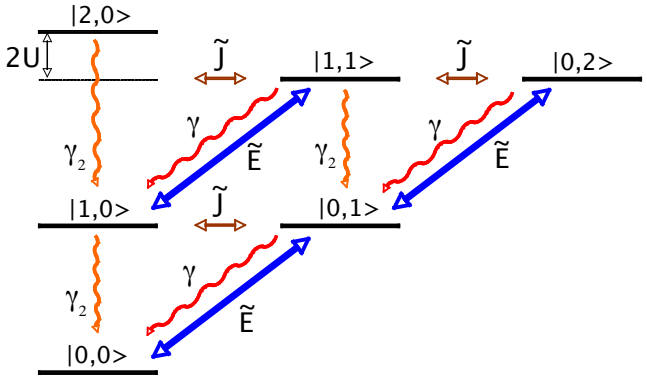

Figure S3: Energy level diagram and rates for the coupled cavity system. The various N_{tot} manifolds are set off from each other by an arbitrary ω_p for visibility. The numbering of the states $|n\rangle$ are from down to up and left to right. For instance $|1\rangle = |1,0\rangle$.

motion are

$$\begin{aligned}
\dot{\tilde{a}}_0 &= 0 \\
\dot{\tilde{a}}_1 &= -\left(i\Delta + \frac{\gamma_2}{2}\right)\tilde{a}_1 - i\tilde{J}\tilde{a}_2 \\
\dot{\tilde{a}}_2 &= -\left(i\Delta + \frac{\gamma}{2}\right)\tilde{a}_2 - i\tilde{J}\tilde{a}_1 - i\tilde{E}\tilde{a}_0 \\
\dot{\tilde{a}}_3 &= -\left(2i\Delta + 2iU + \gamma_2\right)\tilde{a}_3 - i\sqrt{2}\tilde{J}\tilde{a}_4 \\
\dot{\tilde{a}}_4 &= -\left(2i\Delta + \frac{\Gamma}{2}\right)\tilde{a}_4 - i\sqrt{2}\tilde{J}(\tilde{a}_3 + \tilde{a}_5) - i\tilde{E}\tilde{a}_1 \\
\dot{\tilde{a}}_5 &= -\left(2i\Delta + \gamma\right)\tilde{a}_5 - i\sqrt{2}\tilde{J}\tilde{a}_4 - i\tilde{E}\tilde{a}_2
\end{aligned}$$

We have kept terms that are the same order of magnitude in $\frac{|\tilde{E}|}{\tilde{\gamma}}$ and $\tilde{a}_n = a_n e^{i\omega_L t}$ [1]. The steady-state solutions can be easily determined by additionally employing the normalization condition $\sum_{n=0}^{5} |a_n|^2 = 1$ (to order $O(\frac{|\tilde{E}|}{\tilde{\gamma}})^6$) . We find, for $\Delta = 0$,

$$a_1 = -\frac{4\tilde{J}\tilde{E}}{\gamma\gamma_2 + 4\tilde{J}^2}, \qquad a_2 = -\frac{2i\tilde{E}\gamma_2}{\gamma\gamma_2 + 4\tilde{J}^2} \tag{S2}$$

It's interesting to note that in the limit $J/\gamma \gg 1$, $|a_1| \gg |a_2|$, showing that interference effects play an important role. Thus,

$$n_p \sim |a_1|^2 = 16\tilde{J}^2\tilde{E}^2/(\gamma\gamma_2 + 4\tilde{J}^2)^2 \tag{S3}$$

to order $O(\frac{|\tilde{E}|}{\tilde{\gamma}})^4$. Solving for the two-photon manifold amplitudes as well, we find (4)

$$g_2^{(2)}(\tau = 0) \sim \frac{2|a_3|^2}{|a_1|^4} = \frac{\Gamma^2}{\Gamma^2 + 4\alpha^2(\tilde{J})U^2} \tag{S4}$$

[1] Equation (7) in the main text is written in the interaction picture. Here the wavefunction Ψ is the wavefunction written in the Schrödinger picture for completeness.

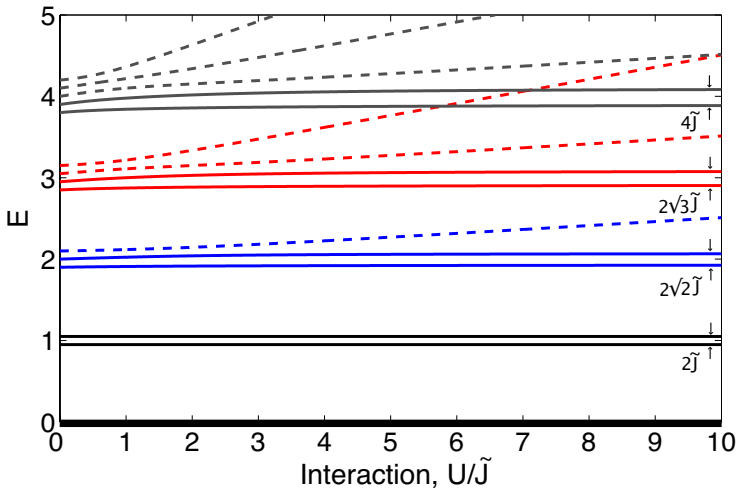

Figure S4: Variation of the energy levels of the three-cavity Josephson interferometer as a function of $U/\tilde{J}$. We plot the first few total photon number manifolds in the range $N_{tot} = 1$ to $N_{tot} = 4$, and $\tilde{J}/\gamma_2 = 0.05$. The various N_{tot} manifolds are marked on the vertical axis and set off from each other by an arbitrary ω_L for visibility. The energy levels in each manifold undergo an anticrossing at $U/\tilde{J} \sim 1$ and a cross-over takes place to an effective Jaynes-Cummings sequence as $U/\tilde{J} \to \infty$.

3 Effective Jaynes-Cummings model

In the limit of ultra-strong interactions, the system of two cavities effectively maps into a Jaynes-Cummings system whose nonlinearity is determined by the tunnel coupling strength. With reference to the hamiltonian (7) in the main text (see Methods section), we show in Fig. S4 how this comes about: two levels of each constant photon-number manifold ($N_{tot} = n_2 + n_s$) split off from the rest of the levels to form a JC-sequence as U is increased beyond $\tilde{J}$.

References

[1] Hartmann, M. J., Brandao, F. G. S. L. & Plenio, M. B. Strongly interacting polaritons in coupled arrays of cavities. *Nature Physics* **2**, 849-855 (2006).

[2] Hennessy, K. *et al.* Quantum nature of a strongly coupled single quantum dot-cavity system. *Nature* **445**, 896-899 (2007).

[3] Faraon, A. *et al.* Coherent generation of nonclassical light on a chip via photon-induced tunneling and blockade. *Nature Physics* **4**, 859-863 (2008).

[4] Andreani, L. C., Panzarini, G. & Gerard, J.-M. Strong-coupling regime for quantum boxes in pillar microcavities: Theory. *Phys. Rev. B* **60**, 13276-13279 (1999).

DOI: 10.1038/NPHYS1223

[5] Combrié, S., De Rossi, A., Tran, Q. V. & Benisty, H. GaAs photonic crystal cavity with ultrahigh Q: microwatt nonlinearity at 1.55 μm. *Opt. Lett.* **33**, 1908-1910 (2008).

[6] Vamivakas, N. *et al.* Strong extinction of a far-field laser beam by a single quantum dot. *Nano Lett.* **7**, 2892-2896 (2007).

[7] Badolato, A. *et al.* Deterministic coupling of single quantum dots to single nanocavity modes. *Science* **308**, 1158 (2005).

[8] Strauf, S. *et al.* Frequency control of photonic crystal membrane resonators by monolayer deposition. *Appl. Phys. Lett.* **88**, 043116 (2006).

[9] Hennessy, K., Högerle, C., Hu, E., Badolato, A. & Imamoglu, A. Tuning photonic nanocavities by atomic force microscope nano-oxidation. *Appl. Phys. Lett.* **89**, 041118 (2006).

[10] Rastelli, A. *et al.* In situ laser microprocessing of single self-assembled quantum dots and optical microcavities. *Appl. Phys. Lett.* **90**, 73120 (2007).

[11] Schuster, D. I. *et al.* Resolving photon number states in a superconducting circuit. *Nature* **445**, 515-518 (2007).

[12] Verger, A., Ciuti, C. & Carusotto, I. Polariton quantum blockade in a photonic dot. *Phys. Rev. B* **73**, 193306 (2006).

[13] El Daïf, O. *et al.* Polariton quantum boxes in semiconductor microcavities. *Appl. Phys. Lett.* **88**, 061105 (2006).